

Selected Paper

Synthesis of Hexagonally Ordered Super-Microporous Silicas, Using Conventional Alkyltrimethylammonium Bromide, as Adsorbents for Water Adsorption Heat-Pump Systems

Kazuhisa Yano* and Yoshiaki Fukushima

Toyota Central Research & Development Labs., Inc., Nagakute, Aichi 480-1192

Received April 14, 2003; E-mail: k-yano@mosk.tytlabs.co.jp

Super-microporous silicas with an ordered hexagonal structure were synthesized under dilute conditions using a conventional alkyltrimethylammonium halide as a template. The d_{100} of the super-microporous silicas was approximately 23 Å. The pore diameter of one of the obtained samples, determined by an argon adsorption measurement, was 16.7 Å. This material adsorbed water vapor with a P/P_0 value higher than 0.29, while desorbing it with a P/P_0 value lower than 0.14. It can be inferred that this super-microporous silica is suitable as an adsorbent for an adsorption heat-pump system.

It has become possible to synthesize mesoporous silicas, such as the M41S family, using a surfactant as a template.[1–3] Although it is possible to control the diameter of the pores by changing the alkyl-chain length of the surfactant when the alkyl-chain length is shortened, a disordered material is usually obtained because of the weakened hydrophobic interaction of the surfactant. Therefore, in general, it is difficult to synthesize a surfactant-templated porous silica with a pore diameter smaller than 20 Å. Meanwhile, in the case of synthesizing a microporous zeolite using an alkylamine template, the upper pore diameter limit is 15 Å.[4–6]

In recent years, attention has been focused on the synthesis of a super-microporous silica with a pore diameter in the range of 10–20 Å, which is intermediate between the range for micropores and mesopores. Super-microporous silica has been expected to function as a shape-selective catalyst as well as a gas separator, for which mesoporous silica is not expected to be suitable. In order to overcome difficulties in synthesizing super-microporous silica by means of conventional synthesis methods using an alkylammonium salt as a template,[7–10] Serrano et al. reported the synthesis of a super-microporous silica with a *d* spacing of 29 Å, adopting a two-step acidic-to-basic process with a cetyltrimethylammonium or dodecyltrimethylammonium salt as the template.[5] Peng et al. synthesized a super-microporous silica with a *d* spacing of 25.5 Å, using a dialkylammonium salt in which one of the methyl groups was substituted with a benzyl group as the template.[11] Also, there has been a report on the synthesis of a super-microporous silica with a *d* spacing of 30 Å, with introduced aluminum into the skeleton using an alkylamine, in place of an alkylammonium salt, as the template.[12] Meanwhile, a super-microporous silica has been synthesized using a bulky organic compound, in place of a surfactant, as the template. Ying et al. synthesized a spherical super-microporous silica with a *d* spacing of 20.4 Å using adamantanamine as the template.[13] Its pore diameter was determined to fall in the range of 13–17 Å, which is almost twice as large as that of adamantanamine, which is approximately 5.9 Å. Marquez et al. synthesized a super-microporous silica having a *d* spacing of 25 Å using a dendorimer as a single-molecule template.[14] However, the super-microporous silicas synthesized by the above-mentioned methods did not exhibit high order diffraction peaks on XRD, indicating ordered materials were not obtained. Bagshaw and Hayman reported the successful synthesis of a super-microporous silica exhibiting high-order X-ray diffraction peaks, using a α-hydroxyalkylammonium halide as the template.[15] However, the *d* spacing of the obtained material was not less than 40 Å, and it is unlikely that a pore with a pore wall thickness greater than the pore diameter can be synthesized when an alkyltrimethylammonium salt is used as the template. Therefore, it is highly likely that the pore diameter of 16 Å obtained with the BJH method could have been an underestimate. Ryoo et al. used short double-chain surfactants as templates to synthesize hexagonally ordered super-microporous silicas with high-order X-ray diffraction peaks with a d_{100} of 29 Å.[6] Although a combination of short double-chain surfactants makes super-microporous silicas remarkably more ordered, short double-chain surfactants have to be synthesized separately, posing a drawback to their wide use.

Meanwhile, because of clean energy, an adsorption heat-pump system has been attracting attention recently. In this system, water is cooled by the evaporation heat when an adsorbent adsorbs water. The adsorbent filled with water is next dried with waste heat. This cycle is repeated to produce a cooled atmosphere. A necessary condition for an adsorbent is adsorption of the greatest amount of water possible at a low relative water pressure. It is anticipated that an ordered porous material with a small pore size is a candidate for an adsorbent for an adsorption heat-pump system.

This report describes the synthesis of a super-microporous silica having an ordered hexagonal structure with a conventional alkyltrimethylammonium halide as the template. It is possible to synthesize a super-microporous silica with an ordered hexagonal structure with a d_{100} of 23.1 Å (pore diameter, 16.7 Å) by optimizing the reaction conditions for decyltrimethylammonium bromide (C_{10}TMABr) and tetramethoxysilane (TMOS). The possibility of its use as an adsorbent for

Published on the web November 15, 2003; DOI 10.1246/bcsj.76.2103

an adsorption heat-pump system is also discussed.

Experimental

Synthesis. C_{10}TMABr and TMOS (Tokyo Kasei), and a 1 M sodium hydroxide solution and methanol (Wako Inc.) were used without further purification. In a typical synthesis, 1.54 g of C_{10}TMABr and 2.28 g of the 1 M sodium hydroxide solution were dissolved in 100 g of a water/methanol (75/25 = w/w) solution. Then, 1.32 g of TMOS was added to the solution with vigorous stirring. After the addition of TMOS, the clear solution gradually turned opaque due to the formation of a white precipitate. After 8 h at continuous stirring, the mixture was aged overnight. The white powder was then filtered out and washed with distilled water at least three times, and then dried at 318 K for 72 h. The obtained powder was calcined in air at 823 K for 6 h to remove any organic species.

Characterization. The calcined samples were stored under a nitrogen atmosphere to prevent water adsorption, with which the peak intensity of X-ray diffraction was largely abolished and the gas adsorption capacity was decreased. X-ray diffraction measurements were carried out with a Rigaku Rint-2200 X-ray diffractometer using Cu-Kα radiation. Nearly 0.2 g of a sample was placed in an X-ray holder in order to obtain a reproducible result (intensity). Nitrogen and argon adsorption isotherms were obtained with a Quantachrome Autosorb-1 at 77 K for nitrogen and 87 K for argon. The sample was evacuated at 423 K under 10^{-3} mmHg before each measurement. The volume at the bending point ($P/P_0 = \sim 0.13$) of the isotherm on a logarithmic scale was adopted as the pore volume, since condensation in super-microporous pores was considered to be over at that point. Water vapor adsorption was measured at 298 K with a Belsorp18 supplied by Bel Japan. The pressure gauge and vacuum line of the Belsorp18 were kept at 373 K to prevent the condensation of water vapor on the inner wall. Each sample was sufficiently hydrated by immersion in water for 12 h. Before each measurement, the sample was evacuated at 298 K under 10^{-3} mmHg. Scanning electron micrograph (SEM) was obtained with a SIGMA-V (Akashi Seisakusho). The surface of sample was coated with gold. Solid-state ^{29}Si MAS NMR spectra were recorded with a Bruker MSL-300WB spectrometer at 59.620 MHz spinning 4 kHz using pulses at 90-s intervals. Thermogravimetric analysis was performed with a Rigaku Thermo-plus under a nitrogen atmosphere, the heating rate being 10 K min^{-1}.

Results and Discussion

1. Synthesis. TMOS Concentration: Synthesis with C_{10}TMABr and TMOS was conducted under conditions similar to those under which STS (Surfactant-Templated Silica) was synthesized using C_{16}TMABr and TMOS.[16,17] First, the effect of the TMOS concentration on the properties of the particles was investigated. Figure 1 shows the X-ray diffraction (XRD) patterns of calcined samples. Diffraction peaks assignable to (110) and (200) planes were not observed, and the intensity of d_{100} was very low for particles synthesized under similar reactant concentrations to the case of STS (Fig. 1(a)). However, as the concentration of TMOS decreased, the peak intensity of d_{100} increased and peaks assigned to (110) and (200) planes appeared, confirming that the materials exhibited ordered hexagonal regularity. The C_{10}TMABr/TMOS molar ratio of the reactant concentrations was 0.127 when the TMOS concentration was 407 mM (Fig. 1(a)). It is obvious from Fig. 1 that ordered materials were obtained with higher C_{10}TMABr/TMOS molar ratios (TMOS concentration of 81.3 mM corresponds to C_{10}TMABr/TMOS molar ratio of 0.63 (Fig. 1(d))). However, the actual C_{10}TMABr/TMOS molar ratios of all of the samples except for that obtained with 407 mM TMOS were approximately 0.15 when they were calculated from the decrease in the thermogravimetry of as-synthesized samples (i.e., a complex of C_{10}TMABr and silicate) (calculated from the mass reduction of as-synthesized samples between 423 K and 873 K). In the case of more hydrophobic C_{16}TMABr, ordered materials were obtained even at a low surfactant/TMOS molar ratio (= 0.127).[17,18] Since C_{10}TMABr is highly soluble in water, it is assumed that C_{10}TMABr in an amount greater than the calculated amount is needed in order to keep C_{10}TMABr inside the honeycomb cage of the as-synthesized material under the synthesis conditions, leading to the formation of an ordered material. The yields of the obtained samples are summarized in Table 1, together with the results of XRD and argon adsorption measurements. Since the yields were around 95%, it is indicated that almost all the TMOS added was converted to the framework of the super-microporous silicas, except in the case of a sample obtained with a TMOS concentration of 407 mM. This supports the above-mentioned reason why an excess amount of surfactant is necessary for the formation of a super-microporous silica.

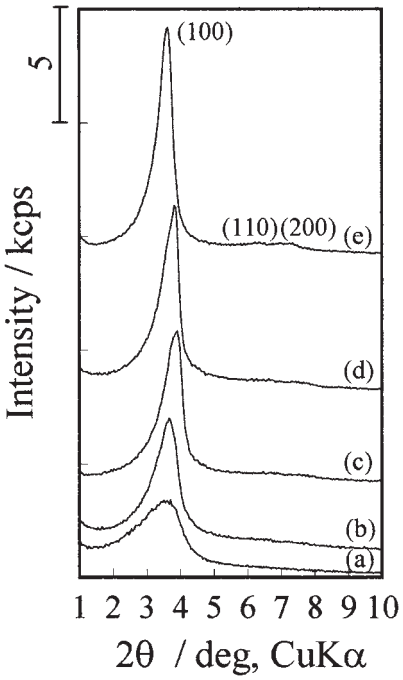

Fig. 1. XRD patterns of calcined samples synthesized with (a) 407 mM, (b) 204 mM, (c) 101 mM, (d) 81.3 mM, and (e) 20.4 mM of TMOS, and 51.5 mM of C_{10}TMABr.

From Table 1, it is obvious that as the intensity of the d_{100} peak decreases, the ordered domain size (calculated from the half width of the d_{100} peak with the Debye–Sherrer equation) and pore volume (determined from the argon adsorption isotherm) also decrease. This indicates that an evaluation of the regularity of the pores using the peak intensity of XRD is appropriate for the obtained samples. The relation between the XRD intensity and the adsorption property is also discussed lat-

Table 1. Dependence of TMOS Concentration on the Properties of Samples

Concentration of TMOS /mM	C_{10}TABr/ TMOS	Yield /%	XRD			Ar adsorption
			d_{100} /Å	Intensity /cps	Ordered domain size[a] /Å	Pore volume /mL g^{-1}
20.4	2.52	95.0	24.4	10181	146	0.38
40.7	1.24	92.6	23.3	8484	—	—
67.5	0.76	95.2	22.8	8174	—	—
81.3	0.63	94.0	23.1	8360	131	0.40
101	0.51	92.3	22.6	6848	113	0.38
136	0.38	91.4	23.3	6556	—	—
204	0.25	97.4	24.1	5994	99.3	0.37
407	0.127	81.9	23.8	3422	56.8	0.24

a) Calculated from half width of d_{100} peak by Debye–Sherrer equation. The values were rather underestimated because of non-crystalline arrangement of silicon and oxygen atoms in the silica wall.

er (in section 3), supporting this indication. Until now, there have been very few studies in which the pore regularity of a porous material was evaluated based on the XRD peak intensity. The reason is related to the difficulty to make reproducible measurements of the peak intensity due to problems with orientation, etc. Since the shapes of samples synthesized in this study were spherical (example in Fig. 2), particles were equally placed in an X-ray holder without any particular orientation, leading to a reproducible result (intensity: with a ±2.5% margin of error).

The peak intensity and d_{100} value were plotted against the TMOS concentration (Fig. 3). d_{100} is minimum and the intensity of d_{100} is high when the concentration of TMOS is within the range of 67.5–101 mM. The corresponding C_{10}TMABr/TMOS molar ratio is 0.76–0.51. The low intensity of d_{100} reveals that disordered materials were obtained with higher concentrations. In such a case, it is assumed that the pore size increased because packing of the hydrophobic parts of the surfactant was imperfect. A perfect arrangement of the surfactant leads to ordered super-microporosity and a small pore size in the range of 67.5–101 mM. However, the pore size was increased by an excessive amount of surfactant with a lower TMOS concentration (20.4–40.7 mM). The C_{10}TMABr/TMOS molar ratio in the latter concentration range was above 1.2, which is more than eight-times greater than the actual amount (0.15).

C_{10}TMABr Concentration: Next, the effect of the C_{10}TMABr concentration on the properties of particles was investigated. Based on the results in Fig. 3, the TMOS concentration was fixed at 81.3 mM, where the d_{100} peak intensity was high, while the d_{100} value was low. The peak intensity and d_{100} value were plotted against the C_{10}TMABr concentration (Fig. 4). The d_{100} value is low (approximately 23 Å) when

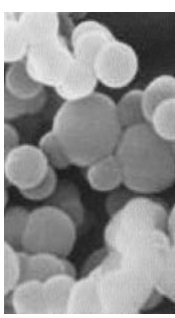

Fig. 2. Transmission electron micrograph of sample synthesized with 81.3 mM of TMOS, and 51.5 mM of C_{10}TMABr.

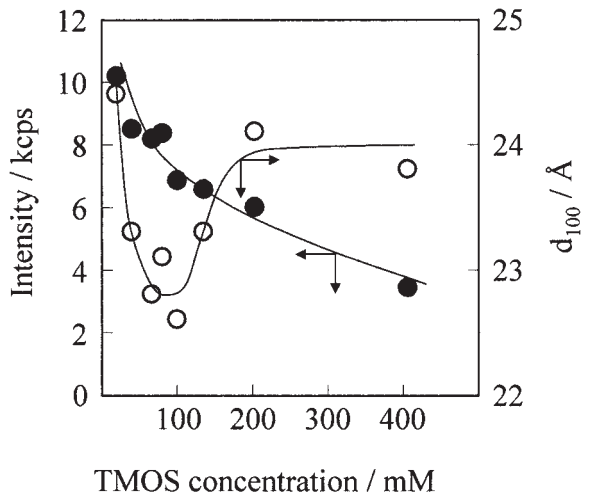

Fig. 3. Effect of the TMOS concentration on the intensity (●) and d_{100} value (○) of samples.

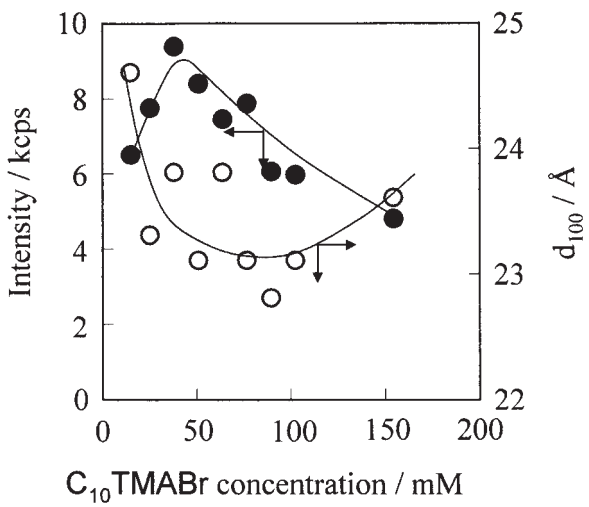

Fig. 4. Effect of the C_{10}TMABr concentration on the intensity (●) and d_{100} value (○) of samples.

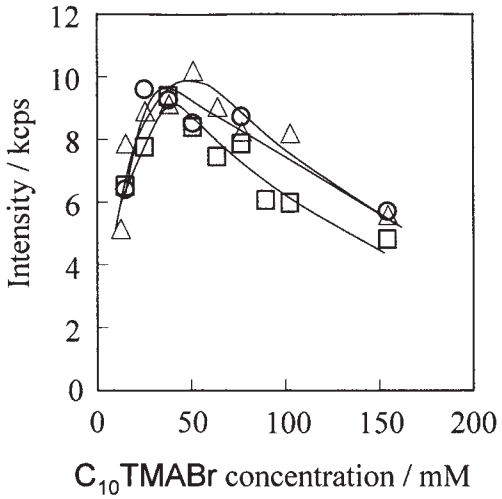

Fig. 5. Effect of the C_{10}TMABr concentration on the intensity of d_{100} of samples synthesized with different TMOS concentrations. (□) 81.3 mM; (○) 40.7 mM; (△) 20.4 mM.

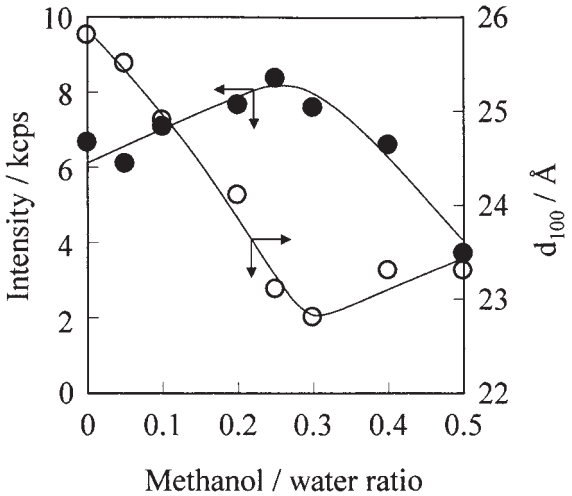

Fig. 6. Effect of the methanol/water ratio on the intensity (●) and d_{100} value (○) of samples.

the concentration of C_{10}TMABr is within the range of 25.8–103 mM. On the other hand, the peak intensity of d_{100} is high when the C_{10}TMABr concentration is within the range of 25.8–77.3 mM.

Another possibility is that the C_{10}TMABr/TMOS ratio may influence the characteristics of the super-micropores. When surfactants are insufficient, a complex of C_{10}TMABr and silicate cannot be adequately formed. On the contrary, when surfactants are in excess, it can be inferred that excess C_{10}TMABr inhibits the formation of a complex of C_{10}TMABr and silicate, which in turn could make the pores less ordered. Accordingly, the TMOS concentration was varied in order to determine whether the C_{10}TMABr/TMOS molar ratio or the C_{10}TMABr concentration affects the properties of super-microporous silica particles. The optimum C_{10}TMABr/TMOS molar ratios were 0.3–0.9, 0.6–2, and 1–4 when the TMOS concentrations were 81.3 mM, 40.7 mM, and 20.4 mM, respectively. As the TMOS concentration becomes lower, the optimum C_{10}TMABr/TMOS molar ratio increases. On the contrary, the optimum C_{10}TMABr concentration is still approximately within the range of 25.8–77.3 mM at any TMOS concentration (Fig. 5). Therefore, the results have clarified that the concentration of C_{10}TMABr, but not the C_{10}TMABr/TMOS molar ratio, determines to what extent pores are ordered.

Methanol Ratio: When STS was synthesized using C_{16}TMABr,[17,18] the pore size decreased as the amount of methanol in the solvent increased. The existence of methanol caused the micelle diameter of C_{16}TMABr to decrease, which in turn brought about a decrease in the pore size of the STS.[17] In this system, it is likely that C_{10}TMABr does not form micelles at the experimental concentration. The concentration of C_{10}TMABr adopted here was 51.5 mM, which was under the CMC (65 mM).[19] An investigation was conducted to determine whether or not the pore size was affected by the amount of methanol in this system. The results are presented in Fig. 6. The intensity of d_{100} increases as the ratio of methanol in the solvent increases, and becomes maximum when the methanol ratio is in the range of 0.2–0.3. On the other hand, the d_{100} value decreases as the ratio of methanol in the solvent increases, and becomes minimum when the methanol ratio is in the range of 0.25–0.3. The pore size was decreased by methanol in a manner similar to at mentioned above. It was also found that the methanol ratio affects the regularity of super-microporosity. As the methanol ratio becomes higher, it takes a longer time until the precipitation of the particles starts, and it can be inferred that the slow rate of the reaction makes the structure more ordered. When the methanol ratio was increased to 0.4 or greater, the intensity of d_{100} decreased. Presumably this is because of an increase in the solubility of C_{10}TMABr with excess methanol, making the agglomeration of C_{10}TMABr more difficult as a result of hydrophobic interactions within the silicate layer.

2. Evaluation of the Pore Diameter. Super-microporous silica with an ordered hexagonal structure was obtained through synthesis under dilute conditions with TMOS and C_{10}TMABr as reactants. The obtained sample exhibited a d_{100} of 23.1 Å when it was synthesized with a TMOS concentration of 81.3 mM and a C_{10}TMABr concentration of 51.5 mM. Next, the pore diameter of this material was evaluated. A nitrogen adsorption isotherm is shown in Fig. 7. The pore diameter was calculated by the BJH method to be 10.4 Å. From the d_{100} value (23.1 Å) obtained by an XRD analysis, the periodic spacing including the wall thickness was calculated to be 26.7 Å. Subtracting 10.4 Å from this value gave 16.3 Å as the thickness of the wall. Compared to a mesoporous silica synthesized using alkyltrimethylammonium as the surfactant, which has been reported to have thick walls of around 10 Å,[1,20] the pores synthesized this time are considered to have a rather thicker wall. In addition, when applying the above pore wall thickness and diameter to a hexagonal structured geometric model, the calculated volume of pores fell below 0.15 g/g, which is substantially less than the actual measured value. The nitrogen adsorption isotherm in Fig. 7 is a type-I adsorption isotherm, in which adsorption to the surface of the pores cannot be distinguished from adsorption resulting from capillary condensation within the pores. In this case, the pore diameter values are presumed to have been underestimated, as adsorption to the surface of the pores was included in the evalua-

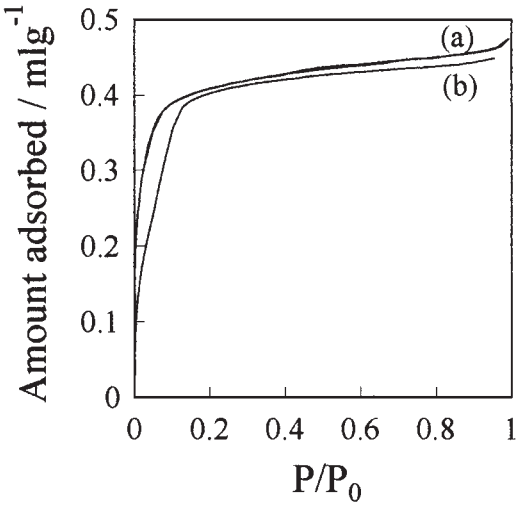

Fig. 7. Adsorption isotherms of super-microporous silica synthesized with 81.3 mM of TMOS, and 51.5 mM of C_{10}TMABr. (a) Nitrogen; (b) argon.

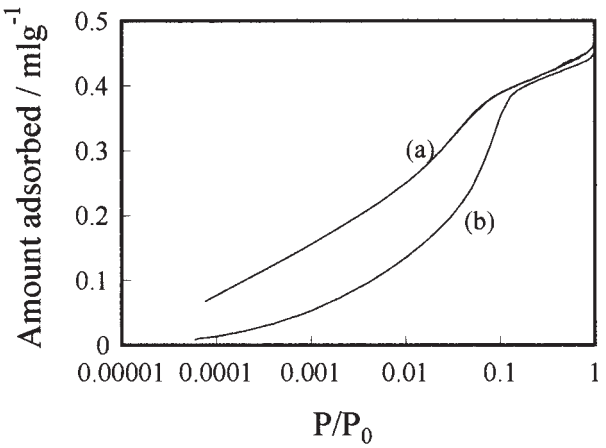

Fig. 8. Adsorption isotherms of super-microporous silica synthesized with 81.3 mM of TMOS, and 51.5 mM of C_{10}TMABr on a logarithmic scale. (a) Nitrogen; (b) argon.

tion.

As a method for determining the diameter of mesopores, an argon adsorption isotherm measurement using the HK method has been proposed.[1,21] An argon adsorption isotherm is also shown in Fig. 7, which allows a slight distinction between adsorption to the surface of the pores and adsorption resulting from capillary condensation. The pore diameter obtained by the HK method is 16.7 Å. In this case, the wall thickness is an appropriate value, i.e. 10 Å.

A great difference was clearly seen between the isotherms on a logarithmic scale (Fig. 8). More nitrogen than argon was adsorbed at very low pressure, and no steep uptake of nitrogen was observed. However, a steep increase was observed for an argon isotherm. It is reasonable to consider that adsorption to the surface of the pores and adsorption resulting from capillary condensation within the pores take place at the same time in the case of nitrogen.

3. Water Vapor Adsorption Properties. One of the most attractive applications of super-microporous silica is as the adsorbent for an adsorption heat-pump system in which cool water is produced by utilizing waste heat. Although zeolites and silica gels have been regarded as candidates for such a system so far,[22] their water adsorption properties are not satisfactory for the requirements of most heat-pump systems.[23] It is preferable for an adsorbent to adsorb a large amount of water vapor at a low relative water vapor pressure ($P/P_0 < 0.3$).[24] Since zeolite adsorbs water vapor at a very low relative water vapor pressure ($P/P_0 < 0.05$), a fairly high temperature is required to dry it. The amount of water vapor adsorbed by silica gel in the preferable range is very small, because it adsorbs water vapor little by little over the whole relative water vapor pressure range owing to the wide pore-size distribution.

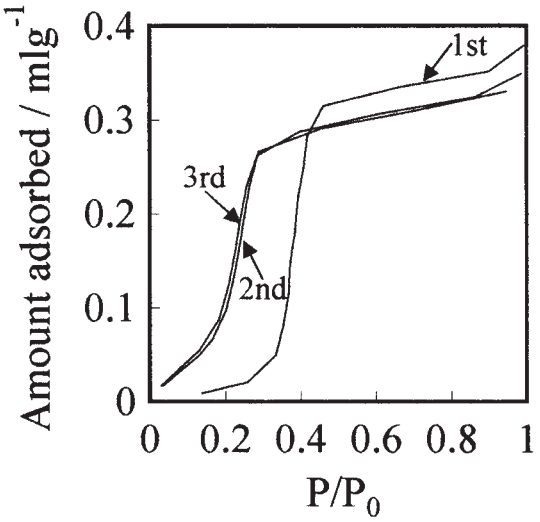

Fig. 9. Water vapor adsorption isotherms of a sample synthesized with 81.3 mM of TMOS, and 51.5 mM of C_{10}TMABr.

Water vapor adsorption isotherms of the super-microporous silica without hydration are shown in Fig. 9. Remarkable differences can be seen in the water vapor adsorption isotherms between the first measurement of the sample, and the second and later measurements. Figure 10 presents NMR charts for a sample after calcination and a water vapor adsorption measurement. After calcination of the sample, only one peak was observed, with peaks Q3 and Q4 overlapping to yield one broad peak. However, after the water adsorption measurement, the Q2, Q3, and Q4 peaks were separated and sharpened, indicating that the surface of the pores was hydrated. This explains the steep increase on the high-pressure side for the first measurement because the surface of the pores was not hydrated; while a water vapor isotherm with good reproducibility was obtained on the second measurement and thereafter because the surface of the pores was sufficiently hydrated. The adsorption volume obtained from the water vapor adsorption measurement was smaller by 0.1 mL/g than the pore volume determined on the nitrogen or argon adsorption measurement. The thickness of the hydrated portion of the surface was calculated to be 1.25 Å from the difference. This value agrees with the thickness calculated assuming that water molecules were adsorbed to all hydroxy groups on the surface of three groups per nm^2.[25–27]

Water vapor adsorption isotherms of hydrated super-microporous silicas synthesized with different TMOS concentrations

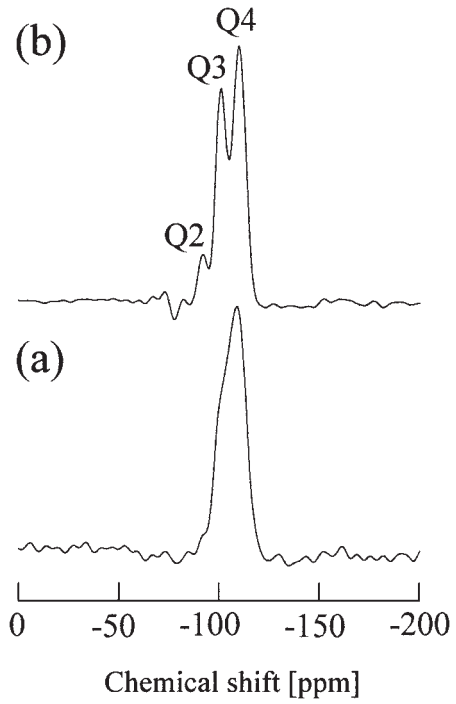

Fig. 10. ^{29}Si-NMR charts of (a) calcined and (b) hydrated samples synthesized with 81.3 mM of TMOS, and 51.5 mM of C_{10}TMABr.

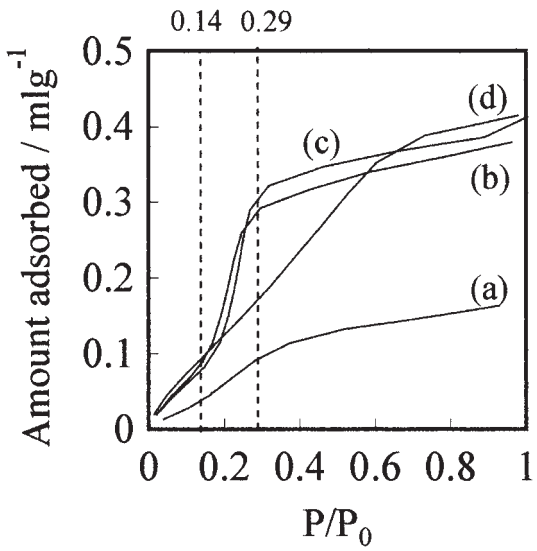

Fig. 11. Water vapor adsorption isotherms of samples synthesized with (a) 407, (b) 81.3, and (c) 20.4 mM of TMOS, and 51.5 mM of C_{10}TMABr. Silica gel (d) adsorbs water vapor gradually over a wide P/P_0 range.

are presented in Fig. 11. The amount of water vapor adsorbed on the material synthesized at the higher concentration (Fig. 11(a)) was very small, and no steep increase in the water vapor adsorption isotherm was observed. However, the materials synthesized at lower concentrations (Figs. 11(b), (c)) adsorbed much water vapor and exhibited a steep uptake. Furthermore, the super-microporous silica with a smallest pore size adsorbed water vapor at a lower relative water vapor pressure (compare Figs. 11(b) and (c)). These results agree well with the results of XRD (Fig. 1).

From Fig. 11, it is obvious that the super-microporous silica synthesized with 81.3 mM TMOS (Fig. 11(b)) adsorbs water vapor at $P/P_0 < 0.3$. There is a steep increase in the amount of water adsorbed between 0.14 and 0.29 (P/P_0), indicating that most of the adsorption–desorption occurs in this range. This material adsorbs water vapor with a P/P_0 value higher than 0.29, while desorbing it with a P/P_0 value lower than 0.14. This material is suitable for use as an adsorbent for a heat-pump system in the case that the temperatures of chilled water–air outside–waste heat are 283–303–343 K, respectively. Since the relative saturated water vapor pressure at 283 K (9.2 torr)–303 K (31.8 torr) is 0.289, water of 283 K could be produced with this material when the temperature of the air outside is 303 K. Furthermore, this adsorbent could be dried with water of only 343 K because the relative saturated water vapor pressure at 303 K (31.8 torr)–343 K (233.8 torr) is 0.136. On the other hand, silica gel adsorbs much less water vapor than the super-microporous silica in the 0.14–0.29 P/P_0 range (silica gel, 0.08 mL/g; the super-microporous silica, 0.22 mL/g), keeping in mind that 2.75 (0.22/0.08) times more silica gel is necessary as an adsorbent compared to super-microporous silica.

It was found that the super-microporous silica adsorbs water vapor at a low relative water vapor pressure ($P/P_0 < 0.3$). Furthermore, when a super-microporous silica has an ordered symmetry, water vapor adsorption occurs in a very narrow pressure range, lowering the water temperature necessary to dry the adsorbent. It can be inferred that a super-microporous silica having an ordered regularity as well as a smaller pore size is suitable as an adsorbent for an adsorption heat-pump system.

Conclusion

It has become clear that it is possible to synthesize super-microporous silicas with an ordered hexagonal structure under dilute conditions using a conventional alkyltrimethylammonium halide (C_{10}TMABr) as the template. The concentrations of TMOS and C_{10}TMABr greatly affect the extent to which and how pores are ordered. The d_{100} value of the super-microporous silica synthesized with 81.3 mM TMOS and 51.5 mM C_{10}TMABr was approximately 23 Å, and the pore diameter calculated from the argon adsorption measurement was 16.7 Å. Argon instead of nitrogen adsorption measurement should be employed for determining the pore diameters of super-microporous silicas, so as to prevent an underestimation of the pore diameter. It can be inferred that super-microporous silicas are suitable as adsorbents for adsorption heat-pump systems.

References

1 C. T. Kresge, M. E. Leonowicz, W. J. Roth, J. C. Vartuli, and J. S. Beck, *Nature*, **359**, 710 (1992).

2 J. S. Beck, J. C. Vartuli, W. J. Roth, M. E. Leonowicz, C. T. Kresge, K. D. Schmitt, C. T.-W. Chu, D. H. Olson, E. W. Sheppard, S. B. McCullen, J. B. Higgins, and J. L. Schlenker, *J. Am. Chem. Soc.*, **114**, 10834 (1992).

3 S. Inagaki, A. Koiwai, N. Suzuki, Y. Fukushima, and K. Kuroda, *Bull. Chem. Soc. Jpn.*, **69**, 1449 (1996).

4 T. Sun and J. Y. Ying, *Nature*, **389**, 704 (1997).

5 D. P. Serrano, J. Aguado, J. M. Escola, and E. Garagorri, *Chem. Commun.*, **2000**, 2041.

6 R. Ryoo, I.-S. Park, S. Jun, C. W. Lee, M. Kruk, and M. Jaronec, *J. Am. Chem. Soc.*, **123**, 1650 (2001)

7 J. S. Beck, J. C. Vartuli, G. J. Kennedy, C. T. Kresge, W. J. Roth, and S. E. Schramm, *Chem. Mater.*, **6**, 1816 (1994).

8 P. T. Tanev and T. J. Pinnavaia, *Chem. Mater.*, **8**, 2068 (1996).

9 M. Kruk, M. Jaroniec, and A. Sayari, *J. Phys. Chem. B*, **101**, 583 (1997).

10 P. L. Ravikovitch, D. Wei, W. T. Chueh, G. L. Haller, and A. V. Neimark, *J. Phys. Chem. B*, **101**, 3671 (1997).

11 Z.-Y. Yuan, W. Zhou, and L.-M. Peng, *Chem. Lett.*, **2000**, 1150.

12 E. Bastardo-Gonzalez, R. Mokaya, and W. Jones, *Chem. Commun.*, **2001**, 1016.

13 T. Sun, M. S. Wong, and J. Y. Ying, *Chem. Commun.*, **2000**, 2057.

14 G. Larsen, E. Lotero, and M. Marquez, *Chem. Mater.*, **12**, 1513 (2000).

15 S. A. Bagshaw and A. R. Hayman, *Chem. Commun.*, **2000**, 533.

16 K. Yano, N. Suzuki, Y. Akimoto, and Y. Fukushima, *Bull. Chem. Soc. Jpn.*, **75**, 1977 (2002).

17 M. T. Anderson, J. E. Martin, J. G. Odinek, and P. P. Newcomer, *Chem. Mater.*, **10**, 311 (1998).

18 M. T. Anderson, J. E. Martin, J. G. Odinek, and P. P. Newcomer, *Chem. Mater.*, **10**, 1490 (1998).

19 R. Satabe and J. Estelrich, *Int. J. Biol. Macromol.*, **28**, 151 (2001).

20 L. Chen, T. Horiuchi, T. Mori, and K. Maeda, *J. Phys. Chem. B*, **103**, 1216 (1999).

21 G. Horvath and K. Kawazoe, *J. Chem. Eng. Jpn.*, **16**, 470 (1983).

22 M. Tather and A. Erdem-Senatalar, *Microporous Mesoporous Mater.*, **34**, 23 (2000).

23 F. Watanabe, A. Kozuka, M. Kumida, and M. Hasatani, *Kagaku Kogaku Ronbunshu*, **19**, 1165 (1993).

24 M. Ito, F. Watanabe, and M. Hasatani, *Kagaku Kogaku Ronbunshu*, **22**, 163 (1996).

25 X. Xie and M. Satozawa, *Microporous Mesoporous Mater.*, **39**, 25 (2000).

26 T. Ishikawa, M. Matsuda, A. Yasukawa, K. Kandori, S. Inagaki, Y. Fukushima, and S. Kondo, *J. Chem. Soc., Faraday Trans.*, **92**, 1985 (1996).

27 X. S. Zhao, G. Q. Liu, A. K. Whittaker, G. J. Millar, and H. Y. Zhu, *J. Phys. Chem. B*, **101**, 6525 (1997).